

## **Supplemental Information**

### **β1 integrin/FAK/cortactin signaling is essential for human head and neck cancer resistance to radiotherapy**

Iris Eke, Yvonne Deuse, Stephanie Hehlhans, Kristin Gurtner, Mechthild Krause, Michael Baumann, Anna Shevchenko, Veit Sandfort, and Nils Cordes

#### **Supplemental Information Inventory**

Supplemental Experimental Procedures

Supplemental References

Supplemental Figure Legends

Supplemental Movies

Supplemental Figures 1 – 25

## Supplemental Experimental Procedures

### *Cell cultures, 3D colony formation assay, radiation exposure and antibody treatment*

Human UTSCC45, UTSCC15, UTSCC14, UTSCC8, UTSCC5, SAS, Cal33, HSC4, XF354 squamous cell carcinoma cell lines of the head and neck (HNSCC) were kindly provided by R. Grenman (Turku University Central Hospital, Turku, Finland). Cells were cultured in Dulbecco's Modified Eagle Medium (PAA; plus glutamax-1) supplemented with 10% fetal calf serum (Biochrom) and 1% non-essential amino acids (PAA). Single doses of 200 kV X-rays (Yxlon Y.TU 320; Yxlon; 0.5 mm copper filter; ~1.3 Gy/min, 20 mA) were applied and measured using a Duplex dosimeter (PTW). To evaluate three (3D)-dimensional clonogenic cell survival, we imbedded cells in Laminin-rich extracellular matrix (IrECM (Matrigel™); BD) as published (1, 2).

### *Integrin analysis by flow cytometry*

The  $\beta$ 1 integrin expression levels were measured by flow cytometry as described previously (3). Staining with AIB2 (non-specific IgG1 as control) was achieved for 30 min on ice followed by labeling with secondary FITC-conjugated IgG antibodies. Finally, prepared cells were resuspended and the FL1 (green fluorescence) was measured using a CyFlow (Partex) equipped with a FloMax 2.4e software.

### *Total protein extracts and Western Blotting*

Cells were harvested using modified RIPA buffer (50 mM Tris-HCl (pH 7.4), 1% Nonidet-P40, 0.25% sodium deoxycholate, 150 mM NaCl, 1 mM EDTA, Complete protease inhibitor cocktail (Roche), 1 mM NaVO<sub>4</sub>, 2 mM NaF) as previously described (1, 2). Samples were stored at -80°C. After SDS-PAGE and transfer of proteins onto nitrocellulose membranes (Schleicher and Schuell), probing of specific proteins was accomplished as published (1).

### *Measurement of apoptosis*

3D cell cultures were treated with AIB2 or IgG#1 (10  $\mu$ g/ml) for 1 h followed by irradiation (0 or 6 Gy). At indicated time points, cells were fixed with 80% ethanol and stained with 4',6-diamidino-2-phenylindole (DAPI; Alexis). At least 100 cells were counted from three independent experiments. Percentage of cells with morphological changes typical for apoptosis was calculated (4).

### Mass spectrometric analysis

After immunoprecipitation, protein mixtures were separated on a gel, in-gel digested with Trypsin and peptides recovered from the gel matrix analyzed on a LTQ Orbitrap XL mass spectrometer (Thermo Fischer Scientific) coupled on-line to Ultima3000 LC system (Dionex) via a TriVersa robotic ion source (Advion BioScience) (1, 5). Database searches were performed by MASCOT software (Martix Science) against HumanIPI database under following settings: mass accuracy 20 ppm and 0.5 Da for precursor and fragment ions correspondingly; enzyme specificity – Trypsin; variable modifications: Methionine oxidated, Cysteine propionamide. Protein hits were then evaluated using Scaffold software (Proteome Software) under following settings: minimal peptide probability 95%, minimal protein probability 99%, and minimal number of matched peptides – two; selected matches were also proved manually.

### Small interfering RNA knockdown

Forty-eight hours after transfection cells were either irradiated (colony formation assay) or lysed for Western blotting.

#### Specific siRNAs used:

siRNA	siRNA ID	Target sequence
hβ1 integrin siRNA	#109878	5'-GGAACCCUUGCACAAGUGAtt-3'
hFAK siRNA	#103698	5'-GGAAAUACAGUUUGGAUCUtt-3'
hSrc siRNA	#683	5'-GGCUGAGGAGUGGUUUUUtt-3'
hJNK1 siRNA	#1415	5'-GGGAUUUGUUAUCCAAAAtt-3'
hJNK2 siRNA	#1452	5'-GGGAUUUGUUUGUGCUGCAUtt-3'
hCTTN siRNA	#146622	5'-CGAAUAUCAGUCGAAACUtt-3'

### FAK expression constructs, FAK site-directed mutagenesis and transfection of FAK plasmids

FAK plasmids were generated as follows: Mouse FAKwt and FRNK fragments were generated by PCR-based amplification from expression plasmids, kindly provided by D.D. Schlaepfer (University of California, San Diego, USA), with specific primers (FAK-N1-fw or FRNK-N1-fw and FAK-N1-rev). Constructs were flanked with *Kpn* I and *Bam* HI restriction sites, and inserted into the *Kpn* I and *Bam* HI sites of pEGFP-N1 (Clontech). Mutation of the FAK activation loop (K578E/K581E) was performed

according to Gabarra-Niecko et al. (6) using appropriate primers (FAKca-fw and FAKca-rev) and the QuikChange II Site-Directed Mutagenesis Kit (Stratagene) according to manufacturer's instructions. Putative Cortactin binding sites were mutated by mutation of two or three proline residues to alanine in the putative Cortactin binding motifs of FAK (FAKmut-CTTN1: P371A/P374A; FAKmut-CTTN2: P642A/P645A/P648A; FAKmut-CTTN3: P873A/P876A/P879A; FAKmut-CTTN4: P973A/P976A). The mutated sites were confirmed by sequencing. Cells were stably transfected with pEGFP-N1 (GFP), FAKwt-GFP, FAKca-GFP, FAKmut-CTTN1-4-GFP or FRNK-GFP expression constructs as published (1). Two weeks after transfection, cells were sorted with a FACScan flow cytometer (BD). Membrane defect cells were excluded by addition of 2 µg/ml propidium iodide per sample.

Specific primers used:

Primer	Mutation	Sequence
FAK-N1-fw		5'-gg-GGTACC-ATGGCAGCTGCTTATCTTGAC-3'
FAK-N1-rev		5'-cg-GGATCC-CG-GCGTGTCTGCCCTAGCATTTT-3'
FRNK-N1-fw		5'-gg-GGTACC-ATGGAATCCAGAAGACAGGCT-3'
FAKca-fw	K578E/K581E	5'-GGAAGACAGTACTTACTATGAAGCTTCCGAAGGAAAATTACC-3'
FAKca-rev	K578E/K581E	5'-GGTAATTTTCCTTCGGAAGCTTCATAGTAAGTACTGTCTTCC-3'
FAKmut-CTTN1-fw	P371A/P374A	5'-GAAGGTGAACGGGCGTTGGCATCAATAGCAAAGTTGGCCAACAGTGAAAAG-3'
FAKmut-CTTN1-rev	P371A/P374A	5'-CTTTTCACTGTTGGCCAACTTTGCTATTGATGCCAACGCCGTTACCTTC-3'
FAKmut-CTTN2-fw	P642A/P645A/P648A	5'-GAAAGATTAGCAATGCCTGCAAATTGTGCTCCCACCCTCTACAGC-3'
FAKmut-CTTN2-rev	P642A/P645A/P648A	5'-GCTGTAGAGGGTGGGAGCACAAATTTGCAGGCATTGCTAATCTTTC-3'
FAKmut-CTTN3-fw	P873A/P876A/P879A	5'-CTGCAGCTCCAGCAAAGAAAGCTCCTCGCGCTGGAGCACCTG-3'
FAKmut-CTTN3-rev	P873A/P876A/P879A	5'-CAGGTGCTCCAGCGCAGGAGCTTTCTTTGCTGGAGCTGCAG-3'
FAKmut-CTTN4-fw	P973A/P976A	5'-GGATGAGACCATTGCTGCTCTTGACGCCAGCACTCATCG-3'
FAKmut-CTTN4-rev	P973A/P976A	5'-CGATGAGTGCTGGCTGCAAGAGCAGCAATGGTCTCATCC-3'

*Transfection of Paxillin-GFP plasmid and time lapse microscopy*

Paxillin-GFP plasmid was a kind gift of A.R. Horwitz (University of Virginia, Charlottesville, USA).

Stably transfected UTSCC15 cells were plated on live imaging dishes. After treatment with IgG#1 or AIB2 Paxillin localization was monitored for 1 h using a LSM 510 Meta (Zeiss).

### *Kinetworks™ Phosphoprotein Analysis*

The authors received detections and densitometric analysis ready-for-publication from Kinexus Bioinformatics Corporation ([www.kinexus.ca](http://www.kinexus.ca)). Detailed information, protocols and the panel of target phosphoproteins and corresponding total protein expression of the Kinetworks™ analysis have been published previously (7) and can also be found at the Kinexus Bioinformatics Corp. website ([www.kinexus.ca](http://www.kinexus.ca)).

### *Proximity ligation assay*

UTSCC15 and SAS cells were grown on cover slips and treated with 100  $\mu$ g/ml AIB2 or control antibody for 1 h. After washing with 1xPBS and fixation with 3% formaldehyde for 15 min cells were permeabilized, blocked and incubated overnight with indicated antibodies. Proximity ligation was performed according to the manufacturer's protocol using the Duolink Detection Kit with PLA PLUS and MINUS Probes for mouse and rabbit (Olink Bioscience; (8)). Samples were analyzed with a confocal microscope (LSM 510 Meta; Carl Zeiss, Inc.) under a 63x oil objective.

### *Mice and in vivo experiments*

Animal facilities and experiments were approved according to the German animal welfare regulations. Immunocompromised 7- to 14-week-old male and female NMRI (nu/nu) mice (Experimental Centre of the Medical Faculty Carl Gustav Carus; Technische Universität Dresden) were further immunosuppressed by whole body irradiation 1 to 5 days before tumor transplantation. We serially transplanted cryopreserved chunks of UTSCC15 tumors onto the back of mice as published (9, 10). For the experiments, pieces of ~1 mm size of second passage tumors with median growth rate were subcutaneously transplanted onto the right hind leg. After reaching a tumor volume of ~100 mm<sup>3</sup> (6 mm diameter), animals were randomly allocated to the different treatment arms. The anti- $\beta$ 1 integrin antibody AIB2 in a volume of 0.3 ml was applied in a dose of 2.5 mg/kg or 10 mg/kg on day 0, 3 and 6. Control animals received PBS or a control antibody directed to ELAV (embryonic lethal abnormal vision) of *D. melanogaster* (anti-ELAV; 10 mg/kg; designated as IgG#2). In the combined treatment arms, a 20 Gy single irradiation dose (200 kV X-rays, 0.5 mm Cu filter; ~1 Gy/min) was applied at day 3 with an interval of 4 hours to the drug treatment. To more specifically measure a radiosensitizing effect of the drug and exclude influences of tumor oxygenation, irradiation was performed under

anoxic conditions using a heavy clamp placed over the proximal thigh of the tumor-bearing leg of anaesthetized mice (120 mg/kg body weight Ketamine [intraperitoneal, i.p.] and 16 mg/kg Xylazine i.p.) 2 min before and during irradiation. (11).

#### *Determination of tumor volume and tumor growth delay*

The tumor diameter was measured twice per week using a caliper (1, 9). Tumor volumes were determined by the formula of a rotational ellipsoid:  $\pi/6 \cdot a \cdot b^2$ , where 'a' is the longest and 'b' is the perpendicular shorter tumor axis. Tumor growth time (GT) was evaluated from growth curves of individual tumors as the time needed after start of the experiment to reach 2 and 5 times the starting volume (GT<sub>V2</sub>, GT<sub>V5</sub>). Medians and standard errors of the medians were calculated for each treatment group, comparisons were performed by Mann-Whitney-*U*-test. Animals were followed up until tumors reached a volume of about 1.5 cm<sup>3</sup>, or until death of the animal. Some tumor did not recur after treatment. These animals were observed over a period of at least 120 days or until death of the animal.

#### *Histology, Immunohistochemistry and Immunofluorescence*

Animals for ex-vivo investigations of the tumors were treated in parallel to the growth delay experiments (9, 10, 12). Unirradiated tumors were removed 4 hours after the second drug treatment at day 3, i.e. at the same time point where irradiation would be performed. Another group of tumors was excised at day 4, 24 hours after irradiation or, for unirradiated tumors 28 hours after the second drug treatment. To determine the proliferative activity of UTSCC15 tumors, 0.1 mg/kg body weight BrdU (10 mg/ml saline) was injected i.p. 1 h before tumor excision. The hypoxia marker Pimonidazole (Natural Pharmacia International) was injected i.p. (0.1 mg/g body weight, dissolved at 10 mg/ml in 0.9% NaCl) at the same time point. Tumors were fixed overnight in 4% formalin and embedded in paraffin. Labeling indices for BrdU and Ki-67 were obtained from 10 randomly chosen viewing fields per tumor section after immunostaining with mouse monoclonal antibodies (anti-BrdU, anti Ki-67 (MIB-1), anti-Pimonidazole) and microwave pretreatment of the sections according to standard procedures. The ARK kit (Dako) was used to suppress unspecific staining of the anti-mouse secondary antibodies. Labeling indices for Ki-67 or BrdU were calculated as the number of positively stained cells divided by the total number of vital tumor cells.

Histological analysis of the micromilieu was performed by an image analysis system. The stained sections were scanned using a Zeiss Axioplan 2 fluorescence microscope (Carl Zeiss) equipped with a scanning stage (Maerzhäuser) and a digital video camera Zeiss Axiocam (Carl Zeiss). The scanning process and subsequent image analysis were performed using KS300 image analysis software (Kontron Elektronik). For evaluation of the hypoxic fraction, masks for necrotic, for vital tumor areas and for Pimonidazole positive areas within the vital areas were drawn. Hypoxic fraction was calculated as the percentage of Pimonidazole positive areas within the vital area. Mitoses were evaluated by morphological criteria in haematoxylin and eosin (H&E) stained tumor sections from 10 randomly chosen viewing fields per tumor section (11). The data for each tumour were derived from a single tissue section. All samples were blinded for analysis.

### Supplemental References

1. Eke, I., Koch, U., Hehlhans, S., Sandfort, V., Stanchi, F., Zips, D., Baumann, M., Shevchenko, A., Pilarsky, C., Haase, M., et al. 2010. PINCH1 regulates Akt1 activation and enhances radioresistance by inhibiting PP1alpha. *J Clin Invest* 120:2516-2527.
2. Storch, K., Eke, I., Borgmann, K., Krause, M., Richter, C., Becker, K., Schrock, E., and Cordes, N. 2010. Three-dimensional cell growth confers radioresistance by chromatin density modification. *Cancer Res* 70:3925-3934.
3. Cordes, N., Seidler, J., Durzok, R., Geinitz, H., and Brakebusch, C. 2006. beta1-integrin-mediated signaling essentially contributes to cell survival after radiation-induced genotoxic injury. *Oncogene* 25:1378-1390.
4. Eke, I., Leonhardt, F., Storch, K., Hehlhans, S., and Cordes, N. 2009. The small molecule inhibitor QLT0267 Radiosensitizes squamous cell carcinoma cells of the head and neck. *PLoS One* 4:e6434.
5. Shevchenko, A., Roguev, A., Schaft, D., Buchanan, L., Habermann, B., Sakalar, C., Thomas, H., Krogan, N.J., Shevchenko, A., and Stewart, A.F. 2008. Chromatin Central: towards the comparative proteome by accurate mapping of the yeast proteomic environment. *Genome Biol* 9:R167.
6. Gabarra-Niecko, V., Keely, P.J., and Schaller, M.D. 2002. Characterization of an activated mutant of focal adhesion kinase: 'SuperFAK'. *Biochem J* 365:591-603.
7. Pelech, S., Sutter, C., and Zhang, H. 2003. Kinetools protein kinase multiblot analysis. *Methods Mol Biol* 218:99-111.
8. Jarvius, J., Melin, J., Goransson, J., Stenberg, J., Fredriksson, S., Gonzalez-Rey, C., Bertilsson, S., and Nilsson, M. 2006. Digital quantification using amplified single-molecule detection. *Nat Methods* 3:725-727.
9. Gurtner, K., Deuse, Y., Butof, R., Schaal, K., Eicheler, W., Oertel, R., Grenman, R., Thames, H., Yaromina, A., Baumann, M., et al. 2011. Diverse effects of combined radiotherapy and EGFR inhibition with antibodies or TK inhibitors on local tumour control and correlation with EGFR gene expression. *Radiother Oncol* 99:323-330.
10. Krause, M., Prager, J., Zhou, X., Yaromina, A., Dorfler, A., Eicheler, W., and Baumann, M. 2007. EGFR-TK inhibition before radiotherapy reduces tumour volume but does not improve local



control: differential response of cancer stem cells and nontumorigenic cells? *Radiother Oncol* 83:316-325.

11. Yaromina, A., Holscher, T., Eicheler, W., Rosner, A., Krause, M., Hessel, F., Petersen, C., Thames, H.D., Baumann, M., and Zips, D. 2005. Does heterogeneity of pimonidazole labelling correspond to the heterogeneity of radiation-response of FaDu human squamous cell carcinoma? *Radiother Oncol* 76:206-212.
12. Krause, M., Gurtner, K., Deuse, Y., and Baumann, M. 2009. Heterogeneity of tumour response to combined radiotherapy and EGFR inhibitors: differences between antibodies and TK inhibitors. *Int J Radiat Biol* 85:943-954.

**Supplemental Figure Legends:**

**Supplemental Figure 1.** (A) Flow cytometric measurement of  $\beta$ 1 integrin cell surface expression of tested cell lines as compared to non-specific IgG isotype controls (mean  $\pm$  SD,  $n = 3$ ). Cells were prepared and measured as described in Materials and Methods. (B) Clonogenic survival of 3D HNSCC cell cultures upon treatment with increasing concentrations of non-specific IgG#2. Data are mean  $\pm$  SD ( $n = 3$ ). (C) Representative images of 3D IrECM colony formation of a  $\beta$ 1 integrin inhibition “responder” (UTSCC15) versus a “non-responder” (SAS) cell line at 8 days after plating. Cells were exposed to 100  $\mu$ g/ml AIB2 or IgG#1 24 h after plating.

**Supplemental Figure 2.** Radiation survival (0 - 6 Gy) of additional 3D grown HNSCC cell lines upon treatment with different AIB2 concentrations as compared to non-specific IgG#1 controls (mean  $\pm$  SD;  $n = 3$ ; t-test; \*  $P < 0.05$ , \*\*  $P < 0.01$ ). Statistics compare AIB2/irradiation versus IgG#1/irradiation.

**Supplemental Figure 3.** (A) Apoptosis of 3D IrECM UTSCC15 cell cultures was determined after treatment with the monoclonal inhibitory anti- $\beta$ 1 integrin antibody AIB2 relative to IgG#1 controls (mean  $\pm$  SD;  $n = 3$ ; t-test; \*  $P < 0.05$ ). Cells were isolated at indicated time points after irradiation and stained with DAPI to detect nuclei with characteristic apoptotic morphology. (B) Whole cell lysates were harvested from 3D IrECM UTSCC15 cell cultures treated with AIB2 or IgG#1 without or in combination with 6-Gy X-rays. Total and cleaved forms of Caspase 3 were measured.  $\beta$ -Actin served as loading control. (C) Densitometry from Caspase 3 cleaved protein bands shown in B is shown upon normalization to total protein. Data show mean  $\pm$  SD ( $n = 3$ ). \*\*  $P < 0.01$ .

**Supplemental Figure 4.** (A) Radiation survival (0 - 6 Gy) of 3D IrECM UTSCC15 cell cultures after treatment with the monoclonal inhibitory anti- $\beta$ 1 integrin antibody mAb13 relative to rat non-specific IgG#1 controls (mean  $\pm$  SD;  $n = 3$ ; t-test). Statistics compare mAb13/irradiation versus IgG#1/irradiation. (B) Clonogenic radiation survival (0 - 6 Gy) of 3D IrECM cell cultures upon siRNA-mediated  $\beta$ 1 integrin knockdown (non-specific siRNA as control). Data show mean  $\pm$  SD ( $n = 3$ ; t-test). Confirmatory Western blot for  $\beta$ 1 integrin depletion. (C) To test AIB2 specificity against  $\beta$ 1 integrin, clonogenic survival was assessed in 2-Gy irradiated,  $\beta$ 1 integrin knockdown 3D cell cultures

exposed to AIB2 or non-specific IgG#1 (mean  $\pm$  SD,  $n = 3$ ; t-test). Co, non-specific siRNA control;  $\beta$ 1,  $\beta$ 1 integrin; n.s., not significant. \*  $P < 0.05$ , \*\*  $P < 0.01$ .

**Supplemental Figure 5.** Time course of the relative volume of UTSCC15 tumors treated with anti- $\beta$ 1 integrin antibodies (AIB2; IgG#2 as control) and irradiation. Accessory tumor volume data sets plotted against time. Comprehensive data sets of tumors treated with either 2.5 or 10 mg/kg of AIB2 or 10 mg/kg non-specific IgG#2 alone or in combination with 20-Gy single dose irradiation (median  $\pm$  SEM of 10 - 18 mice) (see Supplemental Tables 1 and 2).

**Supplemental Figure 6.** Assessment of mitoses in xenograft tumors treated with AIB2 (or IgG#2 control) plus/minus 20 Gy single dose X-rays (mean  $\pm$  SD,  $n = 6 - 8$  per group; t-test). Twenty-eight hours after third antibody (10 mg/kg AIB2 or IgG#2) i.p. injection, haematoxylin and eosin stained tumor samples were analyzed for the number of mitotic cells using 10 randomly selected high-power fields (400-fold magnification) per tumor and plotted as mitosis per mm<sup>2</sup> scale. Arrows indicate mitotic cells. \*  $P < 0.05$ .

**Supplemental Figure 7.** Assessment of BrdU-positivity in tumors upon AIB2 plus/minus 20-Gy irradiation (non-specific IgG#2 as control). Twenty-eight hours after third antibody (10 mg/kg AIB2 or IgG#2) i.p. injection, immunohistochemical analysis of BrdU positive cells among total cells was performed using 10 randomly selected high-power fields (400-fold magnification) per tumor and plotted in percentage scale. Results show mean  $\pm$  s.d. ( $n = 7 - 8$  per group).

**Supplemental Figure 8.** Assessment of Ki-67-positivity in tumors upon AIB2 plus/minus 20-Gy irradiation (non-specific IgG#2 as control). Twenty-eight hours after third antibody (10 mg/kg AIB2 or IgG#2) i.p. injection, immunohistochemical analysis of Ki-67 positive cells among total cells was performed using 10 randomly selected high-power fields (400-fold magnification) per tumor and plotted in percentage scale. Results show mean  $\pm$  s.d. ( $n = 7 - 8$  per group).

**Supplemental Figure 9.** Evaluation of mouse body weight under different treatment regimes. Over time, animal body weight was followed during and after i.p. injection with sterile 1xPBS, IgG#2 (10

mg/kg) or AIB2 (2.5 mg/kg or 10 mg/kg) without or in combination with 20 Gy single radiation dose. Results show mean  $\pm$  s.d. ( $n = 12 - 20$  per group).

**Supplemental Figure 10.** Measurement of tumor areas with necrosis, hypoxia and vital cells.

UTSCC15 tumors were excised at day 4 at 4 or 28 hours after second AIB2 antibody injection plus/minus irradiation. To determine proliferative activity and hypoxia of these tumors, 0.1 mg/kg body weight BrdU (10 mg/ml saline) and 0.1 mg/g body weight Pimonidazole were injected i.p. 1 h before tumor excision. For evaluation of the hypoxic fraction, masks for necrotic, vital tumor areas and Pimonidazole-positive areas within vital areas were drawn. Hypoxic fraction was calculated as the percentage of Pimonidazole-positive areas of total vital area. Results show median of 6 to 8 animals per group. pHF, Pimonidazole-positive hypoxic fraction.

**Supplemental Figure 11.** Analysis of metastases formation. Upon animal scarification at day 120 after start of treatment, organs (liver, kidney, lung, brain; spleen and colon not shown) were examined for macroscopic formation of metastases upon treatment with PBS, IgG#2 (10 mg/kg) or AIB2 (2.5 mg/kg or 10 mg/kg) in combination with 20 Gy single radiation dose. Exemplary organs from mouse #712, #751 and #798 are shown. Examinations were performed in 1 – 8 animals per group.

**Supplemental Figure 12.** Protein kinases with less than 30% change in phosphorylation upon  $\beta$ 1 integrin inhibition. Phosphoproteom array was performed on whole cell lysates of 1h AIB2-treated 3D UTSCC15 cell cultures (IgG#1 as control) (for complete list see Supplemental Table 3). Protein phosphorylation data of selected, sparsely altered prosurvival protein kinase is plotted as fold change after normalization to total protein expression.

**Supplemental Figure 13.** (A) Densitometry of Western blot data shown in Figure 2B. Data show mean  $\pm$  SD ( $n = 3$ ). (B) Western blotting on protein lysates from AIB2-treated 3D cell cultures and UTSCC15 tumor xenografts and detection of p130CAS and Src expression and phosphorylation.  $\beta$ -Actin served as loading control.

**Supplemental Figure 14.** Clonogenic survival of non-irradiated and 2-6 Gy irradiated single Src or JNK2 knockdown cell cultures. Data show mean  $\pm$  SD ( $n = 3$ ). Confirmatory Western blot for Src or JNK2 depletion.  $\beta$ -Actin served as loading control. Co, non-specific siRNA control; S, Src; J, JNK2.

**Supplemental Figure 15.** UTSCC15 cells were stably transfected with FAK wildtype and constitutively active kinase forms tagged to GFP. Upon AIB2 treatment (100  $\mu$ g/ml; IgG#1 as control), cells were fixed 1 h later and stained for FAK Y397 phosphorylation according to Materials and Methods. DAPI was used for nuclear staining. Images were acquired with a confocal microscope (LSM 510 Meta; Carl Zeiss, Inc.) under a 63x oil objective.

**Supplemental Figure 16.** Visualization of changes in Paxillin-positive focal adhesions by AIB2-mediated  $\beta$ 1 integrin inhibition in stably EGFP-Paxillin transfected UTSCC15 cells (see Supplemental Movies 5 and 6). Time lapse microscopy was obtained after a 1-h treatment with AIB2 (or IgG#1 control). Images were acquired with a confocal microscope (LSM 510 Meta; Carl Zeiss, Inc.) under a 63x water objective.

**Supplemental Figure 17.** Densitometry of Western blot data shown in Figure 4B. Data show mean  $\pm$  SD ( $n = 3$ ; t-test). \*\*  $P < 0.01$ .

**Supplemental Figure 18.** Kinetics of FAK-Cortactin dissociation. At 1 h, 4 h, and 24 h, coprecipitation experiments have been performed using anti-FAK antibodies (IgG was used as control) in AIB2-treated 3D UT-SCC15 cell cultures. Densitometry from CTTN protein bands indicates significant reduction of FAK-Cortactin binding over the time period of investigation. Data show mean  $\pm$  SD ( $n = 2$ ; t-test). \*  $P < 0.05$ .

**Supplemental Figure 19. (A)** Western blot analysis of the input of FAK and whole cell lysates for FAK coprecipitation experiments shown in Figure 4D. FAK immunoprecipitation was done from whole cell lysates of AIB2- or TS2/16-( $\beta$ 1 integrin stimulating antibody) treated cells. IgG#1 and IgG#3 served as controls.  $\beta$ -Actin served as loading control. **(B)** Western blot analysis of the input of GFP-FAK and whole cell lysates for GFP immunoprecipitation experiments shown in Figure 4E. GFP

immunoprecipitation was done from whole cell lysates of AIB2-treated (IgG#1 as control) FAK transfectants (FAKwt-GFP, FAKca-GFP, GFP).  $\beta$ -Actin served as loading control. **(C)** Western blot analysis of the expression of GFP-FAK and GFP in GFP immunoprecipitation from whole cell lysates of AIB2-treated FAKca-GFP, FAKwt-GFP and GFP transfectants.  $\beta$ -Actin served as loading control.

**Supplemental Figure 20.** Detection of  $\beta$ 1 integrin expression upon FAK knockdown relative to siRNA controls. Densitometry is shown from indicated Western blots (mean  $\pm$  SD;  $n = 3$ ).  $\beta$ -Actin served as loading control.

**Supplemental Figure 21.** Clonogenic radiation survival of Src and JNK2 knockdown 3D cell cultures exposed to AIB2 and 2 Gy (mean  $\pm$  SD;  $n = 3$ ; t-test; \*\*  $P < 0.01$ ). Co, non-specific siRNA control.

**Supplemental Figure 22.** Western blot analysis on indicated proteins from whole cell lysates of 3D UTSCC15 knockdown cell cultures. Subsequent to single knockdown of FAK, Src, JNK1, JNK2 or Cortactin, cells were treated with AIB2 (or IgG#1 as control) for 1h.  $\beta$ -Actin served as loading control.

**Supplemental Figure 23.** Densitometry of Western blot data shown in Figure 5E. Data show mean  $\pm$  SD ( $n = 3$ ; t-test). \*  $P < 0.05$ , \*\*  $P < 0.01$ .

**Supplemental Figure 24.** **(A)** Western blot analysis of the input of GFP and whole cell lysates for coprecipitation experiments shown in Figure 6C. GFP immunoprecipitation was done from whole cell lysates of 3D grown cells stably transfected with FAK-GFP plasmids expressing FAKwt, FAKmut-CTTN1 (P371A/P374A), FAKmut-CTTN2 (P642A/P645A/P648A), FAKmut-CTTN3 (P873A/P876A/P879A) or FAKmut-CTTN4 (P973A/P976A) or FRNK.  $\beta$ -Actin served as loading control. **(B)** Western blot analysis of the GFP expression GFP immunoprecipitation from whole cell lysates of FAKmut CTTN1-4. **(C)** Densitometry of Western blot data shown in Figure 6D. Data show mean  $\pm$  SD ( $n = 3$ ; t-test). \*  $P < 0.05$ , \*\*  $P < 0.01$ . **(D)** Surviving fraction of 3D grown cells stably transfected with FAK-GFP plasmids expressing FAKwt, FAKmut-CTTN1, FAKmut-CTTN2, FAKmut-CTTN3 or FAKmut-CTTN4 or FRNK. Results show mean  $\pm$  SD ( $n = 3$ ).

**Supplemental Figure 25.** Schematic of how inhibition of  $\beta$ 1 integrin results in radiosensitization via deactivation of a specific signaling pathway involving FAK, Cortactin and JNK1.

**Supplemental Tables****Supplemental Table 1.** Numbers of animals in the different treatment arms.

<b>Antibody (mg/kg)</b>	<b>Irradiation (Gy, single dose)</b>	<b>Number of animals</b>
10 IgG#2	0	16
2.5 AIIB2	0	16
10 AIIB2	0	16
10 IgG#2	20	16
2.5 AIIB2	20	12
10 AIIB2	20	20



**Supplemental Table 2.** Growth of tumors in nude mice upon treatment with AIB2 or IgG#2 plus/minus irradiation (20 Gy single dose). Additional data related to Supplemental Figure 4. Tumor growth time (TGT) is the time needed after start of experiments to reach 2 and 5 times the starting volume (TGT<sub>V2</sub>, TGT<sub>V5</sub>). SE, standard error; n. s., not significant.

Antibody	Irradiation (20 Gy)	Median TGT <sub>V2</sub> (days) [SE]	P-value for AIB2 vs IgG#2	Median TGT <sub>V5</sub> (days) [SE]	P-value for AIB2 vs IgG#2
IgG#2 (10 mg/kg)	0	4 [3;6]		11 [9;29]	
AIB2 (2.5 mg/kg)	0	4 [4;6]	<i>n. s.</i>	13.5 [10;14]	<i>n. s.</i>
AIB2 (10 mg/kg)	0	7.5 [4;10]	<i>&lt; 0.005</i>	23 [13;30]	<i>&lt; 0.03</i>
IgG#2 (10 mg/kg)	20	6 [3;7]		24 [13;56]	
AIB2 (2.5 mg/kg)	20	20.5 [7;31]	<i>&lt; 0.009</i>	56 [28; 108]	<i>&lt; 0.03</i>
AIB2 (10 mg/kg)	20	13.5 [6;18]	<i>&lt; 0.02</i>	38.5 [30; 59]	<i>&lt; 0.07</i>

**Supplemental Table 3.** Phosphorylation ratio of AIB2- versus IgG#1-treated UTSCC15 cells without normalization to total protein amount (additional data not shown in Figure 2A and Supplemental Figure 11).

Protein	Ratio (AIB2/IgG#1)
Double-stranded RNA-dependent protein-serine kinase [T451]	0.6533
Extracellular regulated protein-serine kinase 2 (p42 MAP kinase) [T185+Y187]	0.9161
Extracellular regulated protein-serine kinase 5 (Big MAP kinase 1 (BMK1)) [T218+Y220]	1.5980
Insulin receptor [Y999]	0.2366
Insulin receptor/Insulin-like growth factor 1 receptor [Y1189/Y1190]	0.9360
Kit/Steel factor receptor-tyrosine kinase [Y703]	1.0809
Protein kinase C-related protein-serine kinase 2 [T816]	1.2092
Protein-serine kinase C alpha [S657]	0.7479
Protein-serine kinase C alpha/beta 2 [T638/T641]	1.0644
Protein-serine kinase C beta 2 [T641]	0.7961
Protein-serine kinase C epsilon [S729]	0.7701
Protein-serine kinase C eta [S674]	0.8635
Protein-serine kinase C gamma [T514]	0.8139
Protein-serine kinase C gamma [T655]	1.0670
Yes-related protein-tyrosine kinase [Y507]	0.6475
Adducin alpha (ADD1) [S726]	0.9192
Adducin gamma (ADD3) [S693]	0.6500
B23 (nucleophosmin, numatrin, nucleolar protein NO38) [S4]	0.5894
cAMP response element binding protein 1 [S133]	0.9332
Extracellular regulated protein-serine kinase 1 (p44 MAP kinase) [T202+Y204]	2.1024
Jun proto-oncogene-encoded AP1 transcription factor [S73]	2.3508
Mitogen & stress-activated protein-serine kinase 1 [S376]	0.7665
N-methyl-D-aspartate (NMDA) glutamate receptor 1 subunit zeta [S896]	0.6508
Retinoblastoma-associated protein 1 [S780]	0.9104
Retinoblastoma-associated protein 1 [S807+S811]	1.0150
Signal transducer and activator of transcription 3 [S727]	1.2912
SMA- and mothers against decapentaplegic homologs 1/5/9 [S463+S465/S463+S465/S465+S467]	1.4462

**Supplemental Table 4.** List of hits identified by mass spectrometry in anti-FAK antibody and unspecific control antibody pulldowns from UTSCC15 cells.

N	Protein accession number	Protein	FAK IP		Control	
			Number of matched peptides	Sequence coverage %	Number of matched peptides	Sequence coverage %
1	IPI00012885	pp125FAK	8	8.7	-	-
2	IPI00029601	Cortactin	18	37	-	-
3	IPI00012011	Cofilin 1	9	60	-	-
4	IPI00219365	Moesin	25	45	-	-
5	IPI00843975	Ezrin	11	34	-	-

## Supplemental Movies

**Supplemental Movie 1.** Rounding of UTSCC15 cells after treatment with AIB2. Before imaging, cells were cultured for 24 h. The image acquisition was started when the antibody (100  $\mu$ g/ml) was added to the medium. One image was taken every 30 seconds over a period of 1 h with a Zeiss Axiovert 40 CFL microscope. The movie was assembled from the images using ImageMagick 6.7.2.

**Supplemental Movie 2.** Stable morphology of UTSCC15 cells after treatment with IgG#1. Before imaging, cells were cultured for 24 h. The image acquisition was started when the antibody (100  $\mu$ g/ml) was added to the medium. One image was taken every 30 seconds over a period of 1 h with a Zeiss Axiovert 40 CFL microscope. The movie was assembled from the images using ImageMagick 6.7.2.

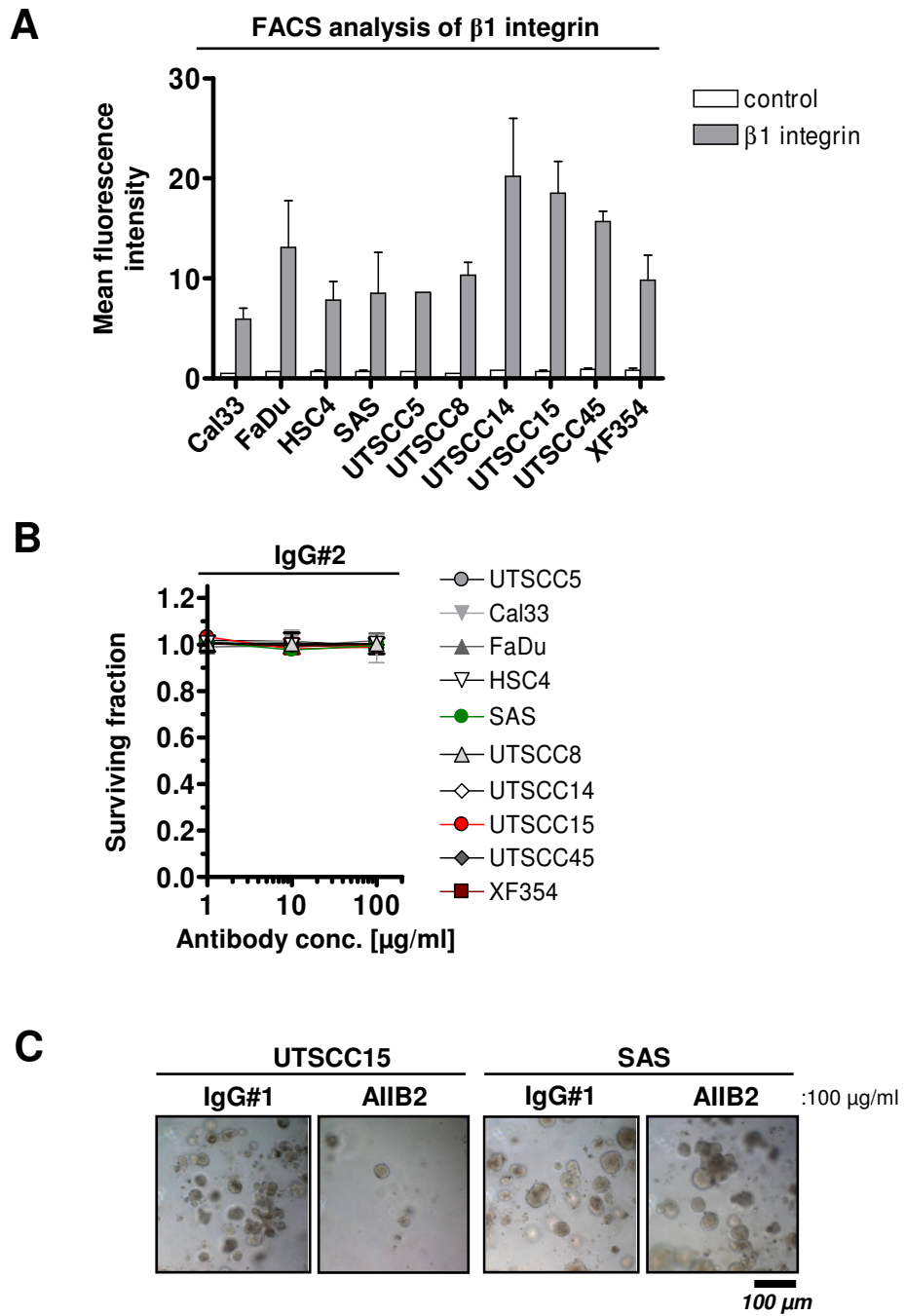
**Supplemental Movie 3.** Stable morphology of SAS cells after treatment with AIB2. Before imaging, cells were cultured for 24 h. The image acquisition was started when the antibody (100  $\mu$ g/ml) was added to the medium. One image was taken every 30 seconds over a period of 1 h with a Zeiss Axiovert 40 CFL microscope. The movie was assembled from the images using ImageMagick 6.7.2.

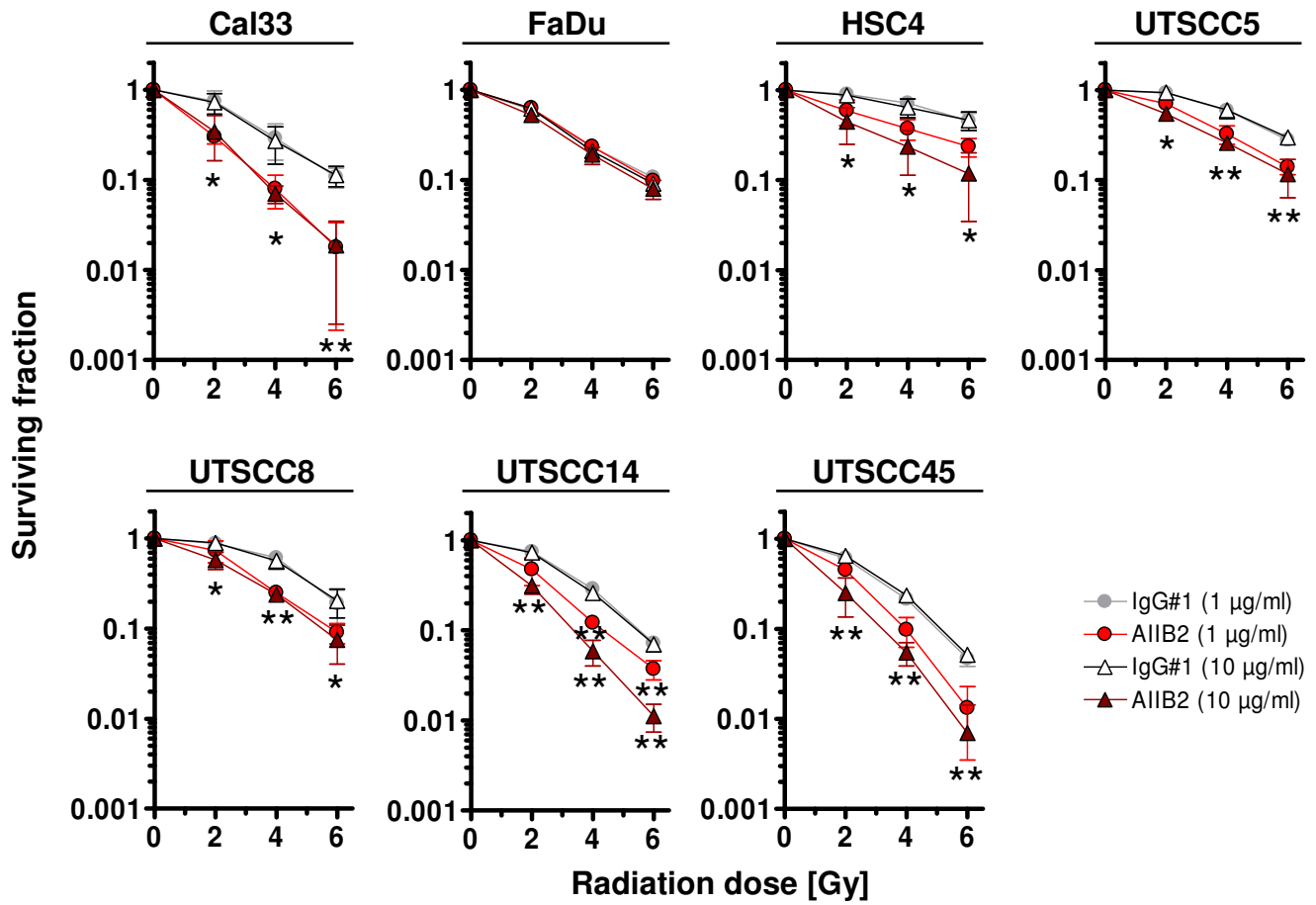
**Supplemental Movie 4.** Stable morphology of SAS cells after treatment with IgG#1. Before imaging, cells were cultured for 24 h. The image acquisition was started when the antibody (100  $\mu$ g/ml) was added to the medium. One image was taken every 30 seconds over a period of 1 h with a Zeiss Axiovert 40 CFL microscope. The movie was assembled from the images using ImageMagick 6.7.2.

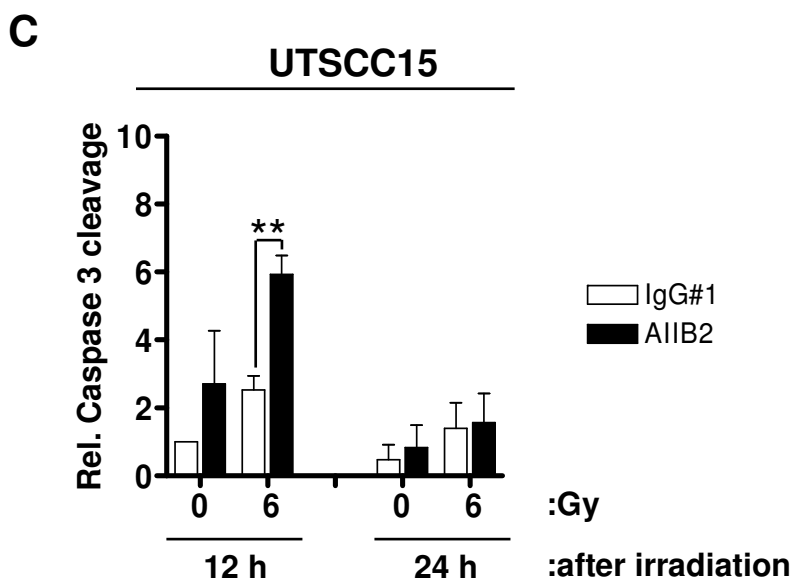
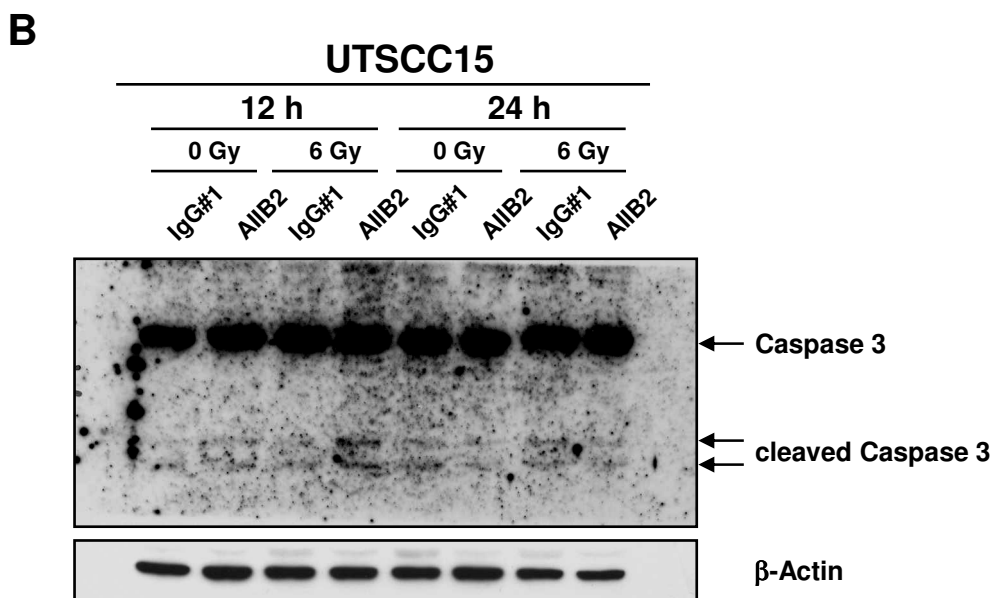
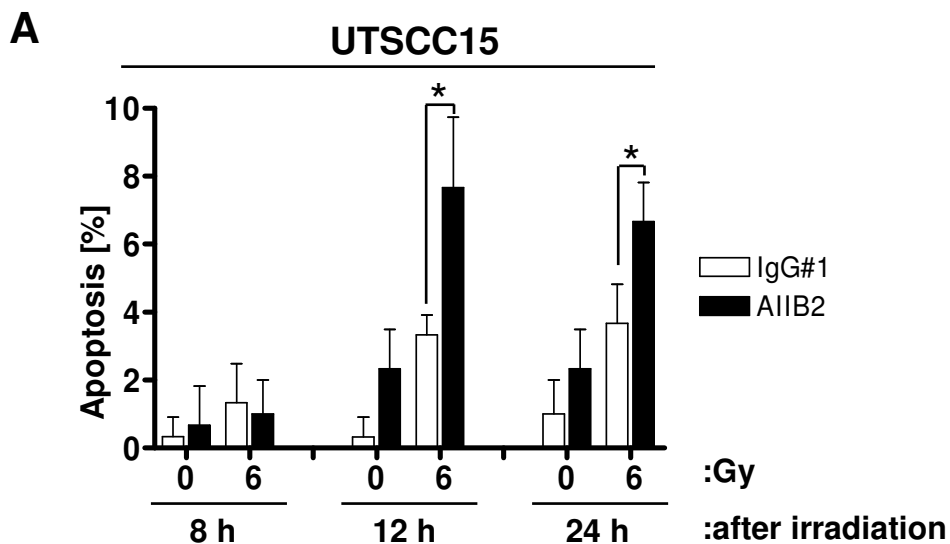
**Supplemental Movie 5.** UTSCC15 cells stably transfected with EGFP-Paxillin showed severe focal adhesion disassembly upon AIB2 treatment. Before imaging, cells were cultured for 24 h. The image acquisition was started when the antibody (100  $\mu$ g/ml) was added to the medium. One image was taken every 10 min over a period of 1 h with a Zeiss Axiovert 40 CFL microscope. The movie was assembled from the images using ImageMagick 6.7.2.

**Supplemental Movie 6.** UTSCC15 cells stably transfected with EGFP-Paxillin showed no changes in focal adhesion assembly upon IgG#1 treatment. Before imaging, cells were cultured for 24 h. The

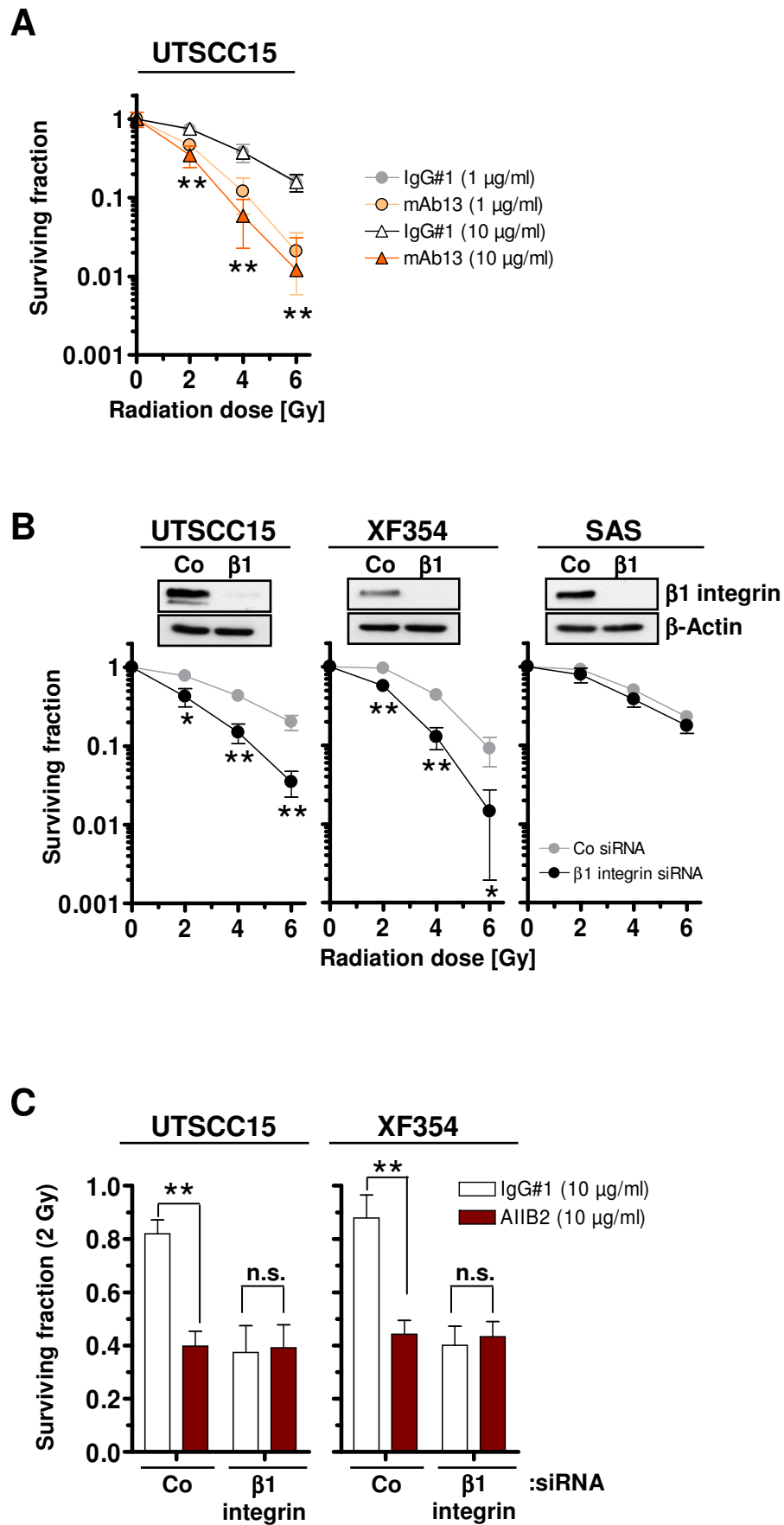
image acquisition was started when the antibody (100  $\mu$ g/ml) was added to the medium. One image was taken every 10 min over a period of 1 h with a Zeiss Axiovert 40 CFL microscope. The movie was assembled from the images using ImageMagick 6.7.2.

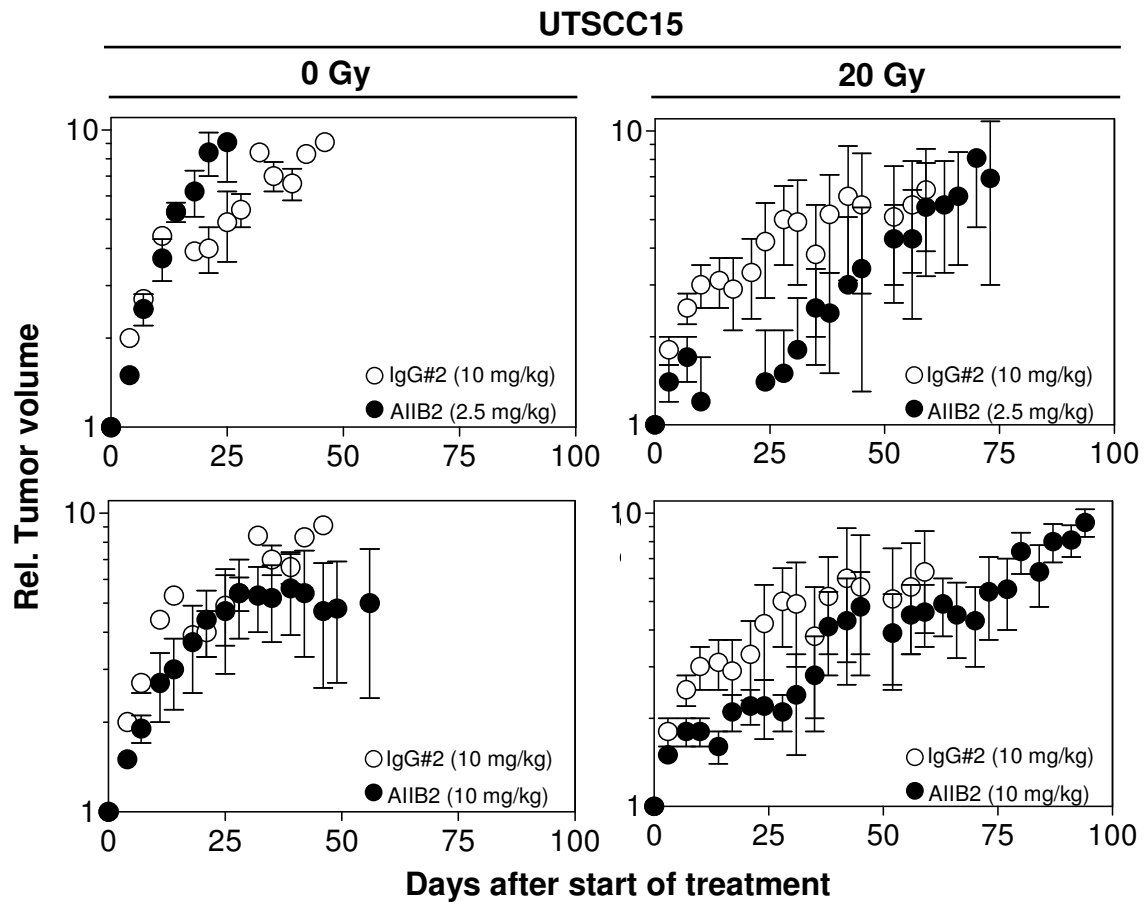


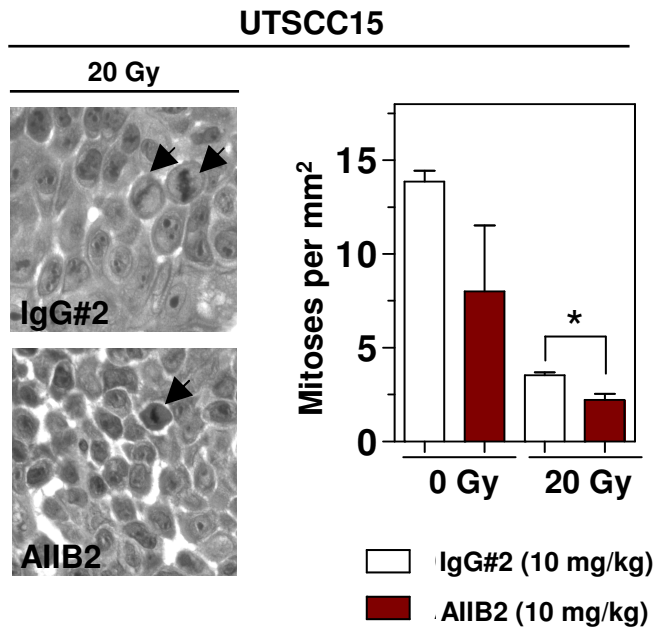


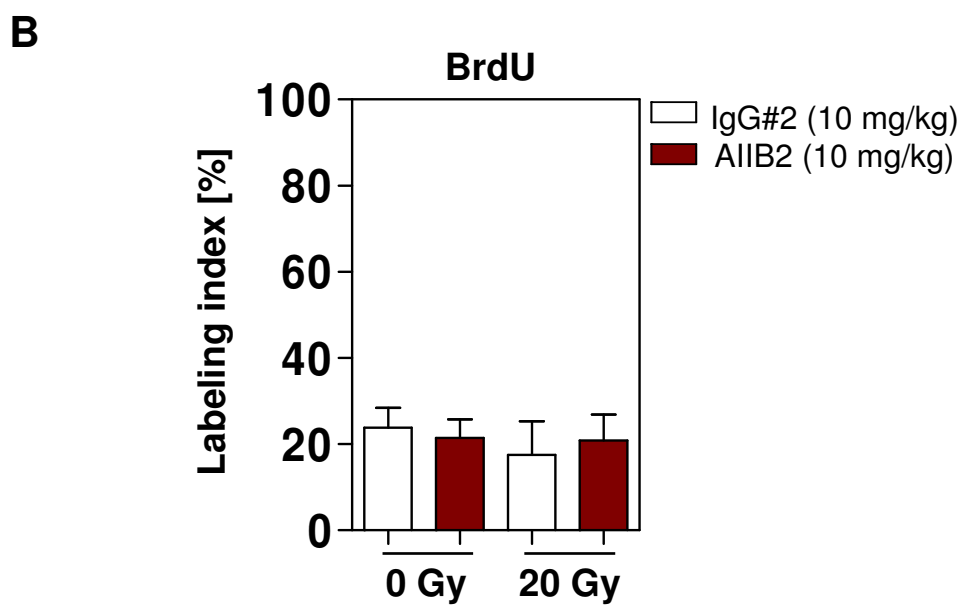
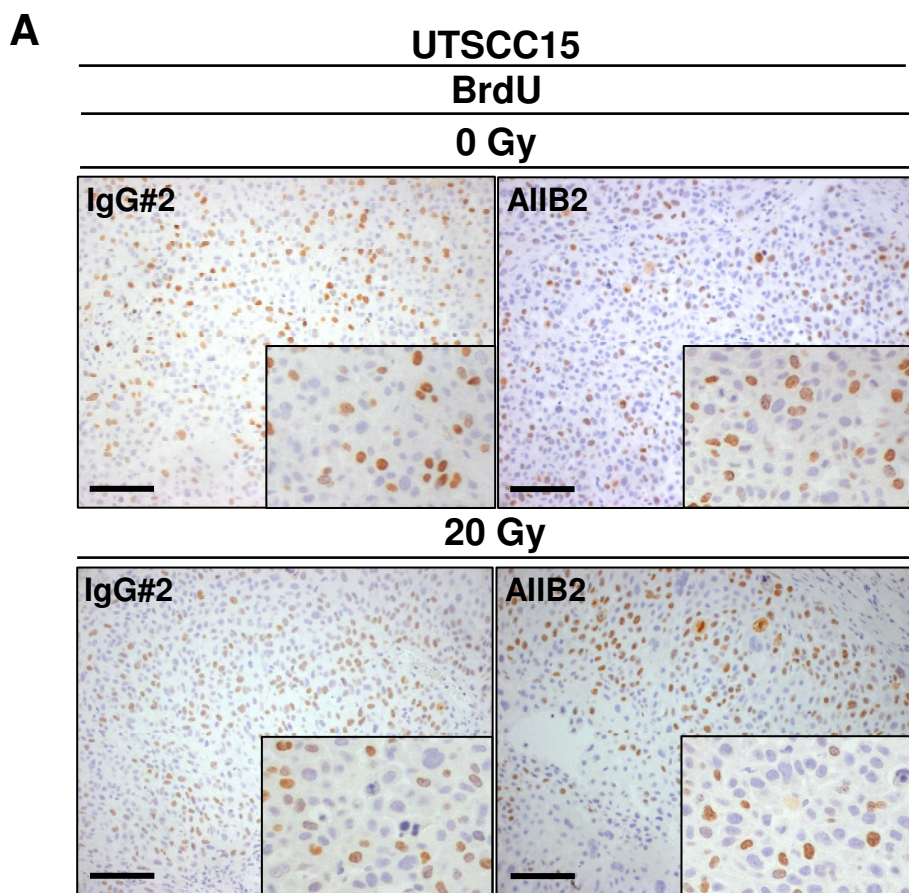


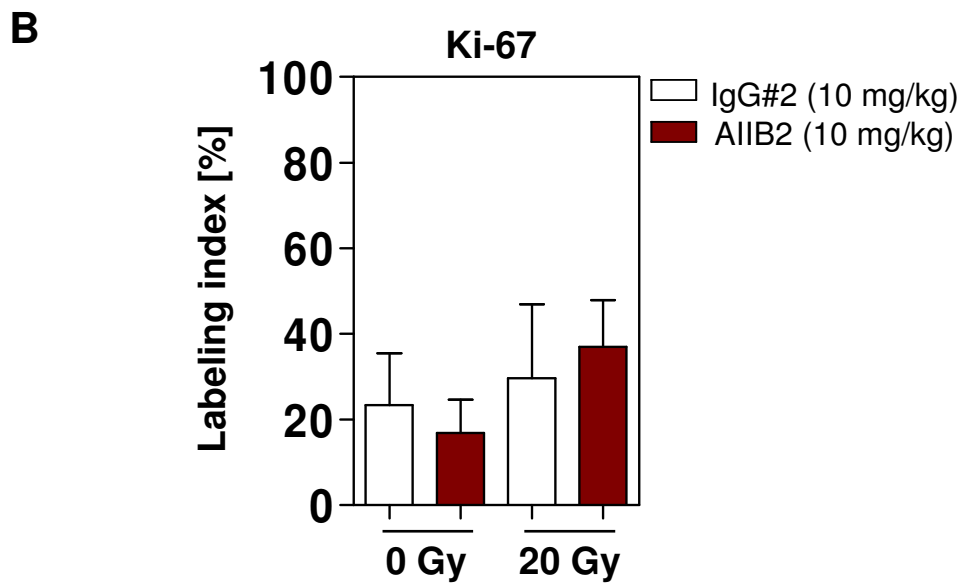
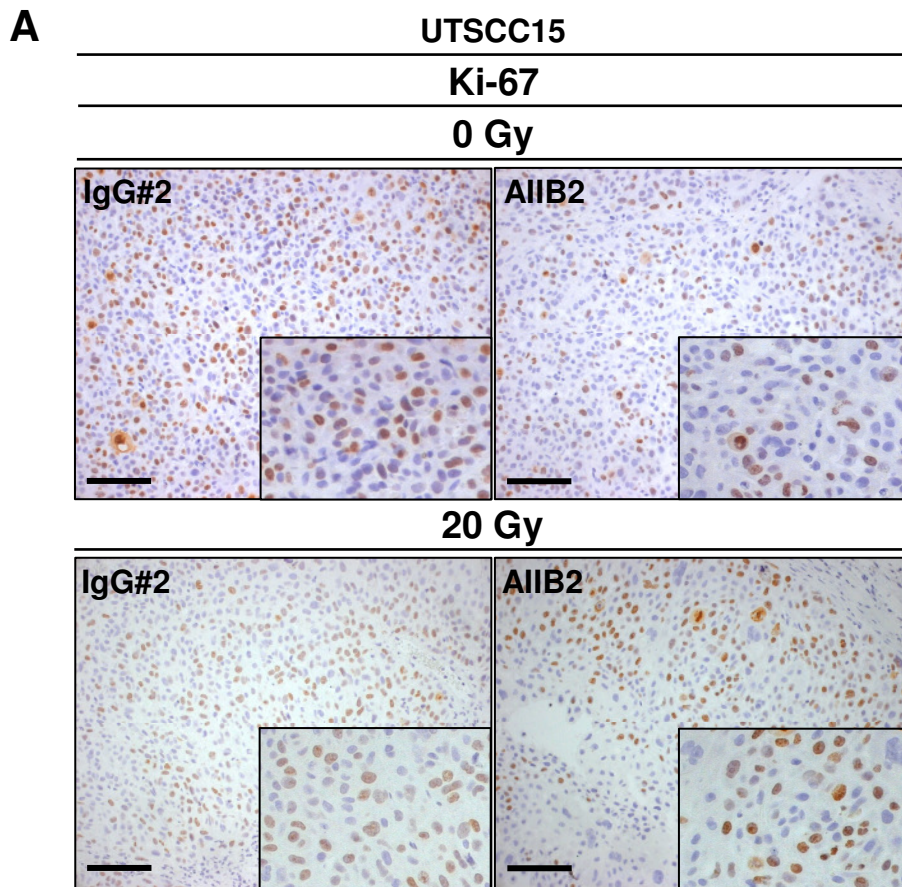


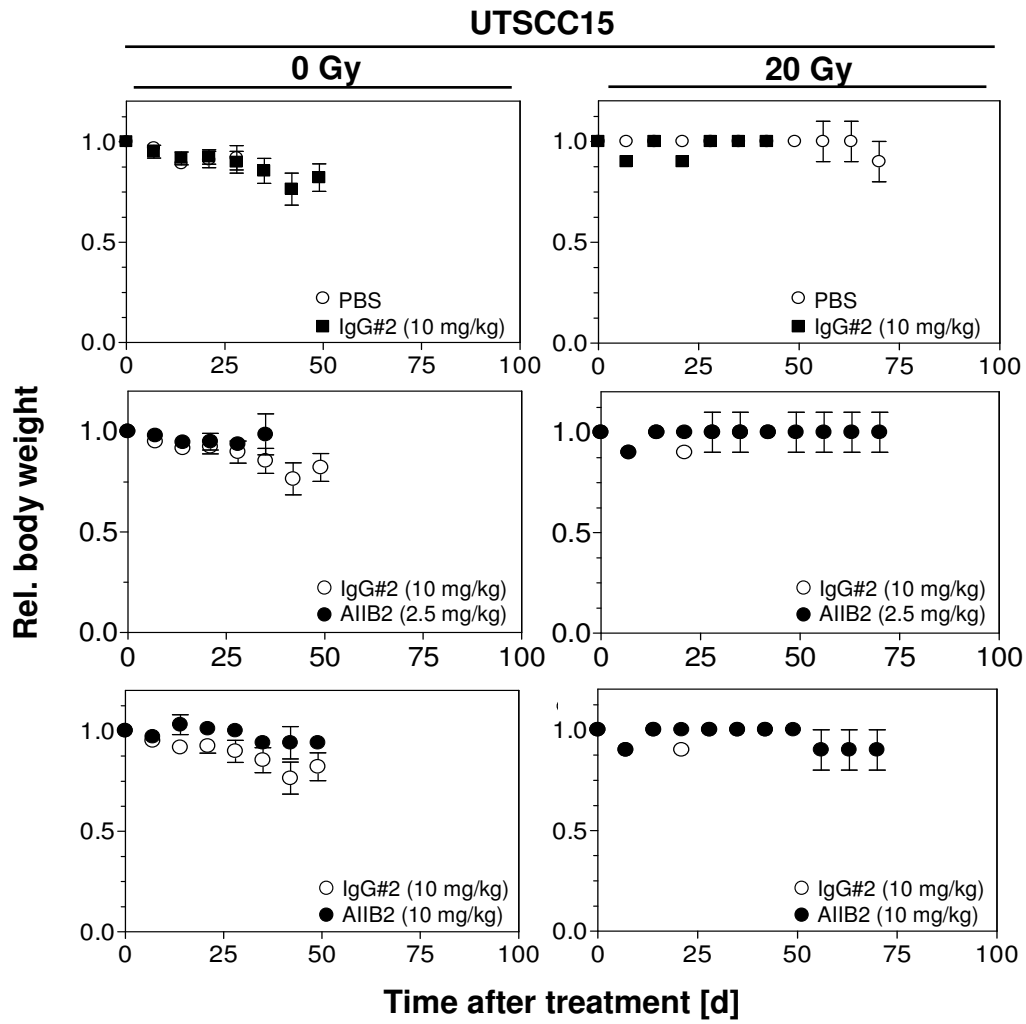












UTSCC15

